

CERN-PRE 89-05.

9

RAL-89-095

Science and Engineering Research Council

# Rutherford Appleton Laboratory

Chilton DIDCOT Oxon OX11 0QX

RAL-89-095

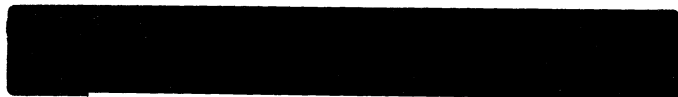


24 OCT. 1989

## HOLRED - A Machine for the Replay of Holograms Made in a Large Bubble Chamber

M Aderholz et al

September 1989



CERN LIBRARIES, GENEVA



CM-P00062900

## **Science and Engineering Research Council**

"The Science and Engineering Research Council does not accept any responsibility for loss or damage arising from the use of information contained in any of its reports or in any communication about its tests or investigations"

HOLRED - A MACHINE FOR THE REPLAY OF  
HOLOGRAMS MADE IN A LARGE BUBBLE CHAMBER

Authors

M Aderholz<sup>6</sup>, P P Allport<sup>5(a),(b)</sup>, J-P Baton<sup>8</sup>, M Bourdinaud<sup>8</sup>,  
G Corrigan,<sup>5(c)</sup> H Drevermann<sup>3</sup>, K K Geissler<sup>3</sup>, J V Gibb<sup>4</sup>, L Gosset<sup>8</sup>,  
G Gros<sup>8</sup>, G Harigel<sup>3</sup>, R Krawiec<sup>1(a)</sup>, J Lloyd<sup>5</sup>, D B Miller<sup>4</sup>, J Moreels<sup>2</sup>,  
D R O Morrison<sup>3</sup>, P R Nailor<sup>4(a)(d)</sup>, M Neveu<sup>8</sup>, J Quidort<sup>8</sup>,  
P Sawallisch<sup>6</sup>, R L Sekulin<sup>7</sup>, S Sewell<sup>7(e)</sup>, G Smith<sup>7</sup>, K Varvell<sup>1</sup>,  
L Verluypen<sup>2(f)(g)</sup>, L Walton<sup>7</sup>, M Waters<sup>7</sup>

- 1 University of Birmingham, B15 2TT, UK
  - 2 IIHE, B-1050 Brussels, Belgium
  - 3 CERN, CH-1211 Geneva 23, Switzerland
  - 4 Imperial College of Science and Technology, London SW7 2AZ, UK
  - 5 Department of Nuclear Physics, University of Oxford OX1 3RH, UK
  - 6 Max Planck Institut für Physik und Astrophysik, D800 München 40, FRG
  - 7 Rutherford Appleton Laboratory, Chilton OX11 0QX, UK
  - 8 CEN Saclay, F-91191 Gif-sur-Yvette, France
- (a) Supported by a grant from SERC
  - (b) Now at Rutherford Appleton Laboratory, Chilton, UK
  - (c) Now with Tessella Support Services Ltd., Abingdon, UK
  - (d) Now with Scientific Generics, Cambridge, UK
  - (e) Now with Autofile Ltd., Slough, UK
  - (f) Also at Universitaire Instelling Antwerpen, B-2610, Wilrijk, Belgium
  - (g) Researcher IIKW, Brussels, Belgium

Abstract

The Fermilab 15' Bubble Chamber, exposed to a beam of neutrinos generated at the Fermilab Tevatron, has been equipped with holographic optics in order to provide a high resolution view of particle interactions over a volume of several m<sup>3</sup>. A machine, "Holred", has been constructed to replay the holograms recorded. The principles of the machine and aspects of its construction and operation are described. Results are presented comparing holographic and conventional recordings of neutrino interactions.

## 1. Introduction: Specification for a Holographic Replay Machine

Recent years have seen a growing interest in the use of holographic optics to record particle interactions in bubble chambers. This technique, originally proposed by Welford<sup>[1]</sup> and also by Russian groups<sup>[2]</sup> in the mid-sixties, received new stimulus after the discovery from 1974 onwards of new particles with lifetimes  $\sim 10^{-13} - 10^{-12}$  s, which, if produced in bubble chamber interactions, would typically travel only a few millimetres before decaying. The study of such short-lived particles by optical means required higher optical resolution than had previously been used in bubble chambers; it has been shown<sup>[3]</sup> that, in order to observe efficiently the decays of particles of lifetime  $\tau$ , resolution  $\lesssim c \tau$  is necessary. Thus resolutions of  $10 \mu\text{m} - 100 \mu\text{m}$  are required for the study of the 'new' particles. The advantage of holography over conventional photography in obtaining resolutions of this order is the decoupling of available resolution from the depth of field offered by the holographic method, and hence the possibility of recording with high resolution over a much larger volume.

The realisation of this advantage led to various projects for the study of the production and decay of short-lived particles in bubble chambers with holographic optics: first, to the use of small chambers, such as the HOBC 1 litre chamber<sup>[4]</sup> at CERN, for the study of charmed particles produced with hadronic incoming beams, and then to the application of holographic optics to large bubble chambers, such as the BEBC chamber<sup>[5]</sup> at CERN and the 15' bubble chamber at FERMILAB, used for the study of neutrino interactions. It should be noted that, while charged particle beams can be focused to a plane, so allowing the use of high resolution optics with conventional photographic recording, typical neutrino beams have diameter  $\sim 1-2$  m at the position of the detection apparatus. It is thus necessary to use a large bubble chamber, (both BEBC and the 15' chambers have useful volumes  $\sim 14 \text{ m}^3$  for the reconstruction of bubble chamber tracks), and to record a substantial fraction of this volume with resolution  $\lesssim 100 \mu\text{m}$ , holography offers essentially the only viable means.

In order to replay bubble chamber holograms in a way useful for subsequent physics analysis of the images obtained, it is necessary to construct specialised machines combining features of conventional bubble chamber scanning and digitising equipment with the optical demands made by the use of holography.

Such machines<sup>[6]</sup> were constructed to replay holograms made in the small bubble chamber HOBC, referred to above. The design of a machine to replay holograms made in a large bubble chamber presents additional problems due to the very different scale involved; thus the specification for a machine to replay holograms made in the FERMILAB 15' chamber contained the following requirements:

- The machine must reconstruct objects over the whole volume in which holographic images were recorded. In the original bubble chamber space this represents a volume of linear dimensions  $\sim 4 \text{ m} \times 2 \text{ m} \times 2 \text{ m}$ .
- Accurate location of images in the reconstructed space must be possible. This means that digitised stages must be provided in three dimensions with a range of travel equal to the size of the reconstructed image space. The object to image magnification is in principle itself a parameter of the machine design; as will be seen from the discussion in subsequent sections, optimisation of the optical design led to a choice of an object to image demagnification by a factor  $\sim 2$ , so that the region over which accurate image digitising must be provided has linear dimension  $\sim 2 \text{ m}$ .
- Images must be reconstructed with the highest possible resolution. This means that the whole of the wavefront recorded from any object must be used in reconstructing the image. In addition, any aberrations of the wavefront recorded on the hologram must be corrected, and no new aberrations introduced. These last considerations very largely determine the optical design of the machine.
- The machine must be capable of handling large numbers of holograms. Most bubble chamber experiments produce large amounts of film, from which interesting physics results are extracted after scanning and measuring substantial numbers of events. In the case of the neutrino experiments for which the present machine was intended, the number of holograms containing an event of potential interest is  $\lambda 10^5$ . The holograms are recorded on reels of film, each containing about 1,000 holographic exposures.

- Some computer control of the machine must be provided. In particular, it should be possible to drive the digitised stages to any desired point in the reconstructed image space in order to examine events which have known space coordinates, as they have been seen on the conventional bubble chamber photographs which are taken at the same expansion of the chamber. In addition, attachment to a computer with data storage facilities will clearly aid fulfilment of the batch processing requirement described above, by providing computerised book-keeping facilities.
  
- Finally, a provision is required to make a photographic recording of the reconstructed image of any event of interest. While this is not an essential requirement of a holographic reconstruction machine - (images can, for instance, be projected onto a vidicon and viewed on a TV monitor) - it enables the four conventional (lower resolution) photographs taken on each expansion of the chamber to be supplemented by a high resolution recording of interesting events, regardless of the position of the event in the bubble chamber. These five photographic views can then be examined on conventional bubble chamber projection apparatus and further physics studies carried out.

This paper describes a machine, 'HOLRED' (HOLographic REplay Device), designed and constructed to fulfil the specification outlined above. The machine, which is sited at Rutherford Appleton Laboratory, was designed by members of a consortium of groups (Birmingham, Brussels University, CEN Saclay, CERN, IC London, MPI Munich, Oxford University and Rutherford Appleton Laboratory) participating in an experiment, (E632), in which the FERMILAB 15' bubble chamber was exposed to a wide-band neutrino beam generated at the Fermilab Tevatron, and was intended to provide a regional centre for holographic analysis. Reports are available on two other machines of independent design<sup>[7]</sup> which have been constructed to provide a holographic replay facility for other experimenters at the 15' bubble chamber, and machines have also been devised for replay of holograms from the (somewhat smaller) MIT-Tohoku 1m<sup>3</sup> bubble chamber<sup>[8]</sup> exposed to the same neutrino beam at Fermilab. A preliminary discussion of the design criteria for HOLRED has been reported previously<sup>[9]</sup>.

The rest of this paper is arranged as follows: Section 2 contains a brief description of the method used to obtain holograms in the FERMILAB 15' bubble chamber, and of the method used to analyse the data, both photographic and holographic. In Section 3 the optical design of the machine is discussed and Section 4 contains a description of its mechanical, electrical and control aspects. In the final section, the overall performance of the machine is described and its relation to other work involving holographic visual inspection is briefly mentioned.

## 2. Recording and Analysis of Interactions in the FERMILAB 15' Bubble Chamber

### 2.1 Holographic Recording

The method used to make holographic recordings of particle interactions in the FERMILAB 15' bubble chamber has been described in detail elsewhere<sup>[10]</sup>. We give here only a general description of the method, emphasising those aspects which bear a strong relation to the subsequent reconstruction of holograms.

The method is illustrated in Figure 1. The chamber was illuminated by light from a pulsed ruby laser ( $\lambda = 694 \text{ nm}$ ), fired about 1 ms after the entry of the particle beam from the accelerator, so that bubbles formed at that time have grown to the desired size ( $\sim 100 \mu\text{m}$  in diameter). The collimated beam of light, entering at the bottom of the chamber, passed through a diverging lens. This lens serves both as entry window and as the means of separating the holographic reference and object beams which must subsequently interfere in order to form the hologram. Reference light, travelling along the optic axis of the lens, passed through the fisheye lens (consisting of three concentric hemispherical glass or quartz shells) situated near the top of the chamber, and encountered the holographic film at normal incidence. The film was sucked down against a gate situated at the centre of the fisheye. Light leaving the entrance lens at angles other than  $0^\circ$  provided the object illumination. Light scattered by bubbles in the direction of the holographic camera passed through the fisheye lens and interfered with the reference light, forming the holographic recording on film. In order to compensate for the fact that the light scattered per unit solid angle from a bubble falls off very rapidly as the scattering angle increases, the entrance

lens had a highly aspheric design, refracting much more light per unit solid angle at large angles with respect to the lens axis than at small angles, (a factor of  $\sim 1,000:1$  between  $0^\circ$  and  $20^\circ$ ).

The exact position of the holographic film with respect to the fisheye was defined by three camera-based fiducial marks whose imprint was recorded on the film at three corners of the region exposed holographically. In addition, at the time of exposure, the film was clamped against an optically flat glass.

In Figure 1 some of the other fisheye lenses, containing conventional photographic cameras, are shown, as well as a section through the 'fiducial volume', the volume within which particle interactions must lie if accurate stereoscopic reconstruction of tracks coming from the interactions is to be achieved from the conventional photographs. The conventional cameras recorded the same events as did the holographic camera, but were exposed later during the bubble chamber expansion cycle, when the bubbles had grown to a larger size. Of the 4 conventional cameras, one had resolution  $\sim 200 \mu\text{m}$  and recorded bubbles of this size over a depth of  $\sim 1 \text{ m}$ , and the others had resolution  $\sim 400 \mu\text{m}$  and recorded in the whole fiducial volume. The aim of the holographic system was also to provide holographic recording of the whole of the fiducial volume ( $\sim 14 \text{ m}^3$ ); this implies that  $\theta_{\text{max}}$ , the half-angle of the cone into which light is dispersed by the entrance lens, must be  $\sim 40^\circ$ .

One further point should be noted concerning the design of the holographic system, namely that both reference and object beams pass through the hemispherical fisheye lens, so the wavefronts arriving at the film suffer from quite severe spherical aberration. (In holographic practice it is quite common to record an aberrated object wave front, but it is unusual to use an aberrated reference beam). It is necessary to compensate for this fact in replaying the hologram, otherwise resolution is lost.

## 2.2 The use of Conventional Photographic Recordings and Holographic Recordings in the Film Analysis

The first part of the analysis of the film from the experiment followed normal bubble chamber practice, namely the scanning of the conventional photographic views for neutrino-induced interactions, and the stereoscopic reconstruction of at least two such views to provide information on the interaction point in the chamber.



HOLRED was therefore designed on the assumption that the positions of interesting particle interactions in the bubble chamber were known before starting analysis of the holographic film. When the corresponding holographic view was required, the hologram was replayed on HOLRED and the stage carrying the vidicon camera was driven straight to the appropriate point in the reconstructed image space in order to view the holographic image.

### 3. Considerations Determining the Optical Design of HOLRED

The principles of the method used to provide the precision reconstruction of events required by HOLRED are shown diagrammatically in figure 2. The design was dominated by two main considerations: first, to provide a real (rather than virtual) image, which would be projected onto a viewing device such as a vidicon camera; and second, to provide optics which minimised the aberrations in the reconstructed image. These aims were achieved by using an exact time-reversed version of the original reference beam to replay holograms, and by supplying, as far as possible, identical optics in the path of the replayed image beam to those present in the bubble chamber, so that the image light retraces its original path through the aberrating elements, and the aberrations are removed. This also implies use of the same wavelength of light for replay. This method of aberration correction by phase conjugated replay is a well-known holographic technique<sup>[11]</sup> and was applied in practice by positioning the hologram at the centre of a 3-component fisheye lens, identical to the one in the bubble chamber, so that its position with respect to the fisheye is identical to that of the film in the bubble chamber camera relative to the bubble chamber fisheye. Raytracing studies indicated that, in order to ensure that aberrations in the image, (represented by the disc of least confusion), should be less than 50  $\mu\text{m}$ , the film must be positioned to within  $\sim 35 \mu\text{m}$  of its original position with respect to the fisheye in the direction perpendicular to the fisheye axis; in the mechanical design, provision was made for such fine-positioning adjustments. The replayed wavefront at the final fisheye surface is then aberration-free. At this point, however, it is no longer possible to provide exact time-reversed optics, because the image is replayed into air, whereas the object space in the bubble chamber contained a liquid hydrogen-neon mixture with refractive index  $\sim 1.1$ . The method used to compensate for this refractive index change in replay is described in Section 3.2 below. First, however, we give some details of the optics of the replay beam.

### 3.1 Replay Beam Design and Replay Laser

As mentioned in Section 2.1, the reference beam incident on the film in the bubble chamber camera passed through the fisheye lens, and so contained substantial spherical aberration. This must be reproduced in the time-reversed replay beam in order that the diffracted image beam should itself be the exact time-reversed version of the recorded object wavefront. The required converging and aberrated replay beam was obtained with a two-component lens system consisting of a commercial diffraction-limited achromat and a concavo-convex 'aberrator' lens separated by  $\sim 10$  mm. The characteristics of the aberrator lens were designed by computer optimisation so that rays traced through the doublet (placed  $\sim 30$  mm before the film) and the fisheye into a medium of refractive index of the chamber liquid came to a focus at a distance equal to the original laser entry point from the fisheye. In the optimised design, this focal spot had diameter  $\sim 25 \mu\text{m}$ , thus ensuring, (in the approximation of far-field optics), that aberrations in the reconstructed bubble images should not exceed this amount [12]. The design of the aberrator lens placed quite strict tolerances on its manufacture, with the requirement that the radii of curvature of the lens be within  $\sim 0.1\%$  of their nominal values; however, within these tolerances, errors could be compensated by slightly adjusting the distance between the two components of the doublet. In setting up the replay beam, the spot was focused onto a vidicon placed at the desired distance from the fisheye, and the optical components adjusted so that aberrations in the spot image were minimised.

In order to provide a replay beam of the same wavelength as that of the pulsed ruby laser with which the hologram were made, a dye laser was used, pumped by an argon ion laser giving an output of 4 W on all lines. The dye laser, (a Spectra Physics model 375B), gave output power of  $\sim 250$  mW at a wavelength of 694.3 nm using DCM dye dissolved in propylene carbonate and was equipped with an ultra fine etalon. This power gave sufficient image intensity in the replayed image beam for bubble images recorded with a ratio  $B$  of object to reference light intensity,  $B \gtrsim 10^{-7}$ , to be visible when projected onto a high sensitivity vidicon camera, and for photographic recordings of the replayed image to be made (using film sensitive at the far red end of the visible spectrum) with reasonable exposure times, (typically  $\lesssim 1$  s). It may be noted that the intensity in the replayed image can be very small for recordings made using the technique described in Section 2.1. This

arises because the light diffracted into the holographic image is proportional to the product  $\{|R| \cdot |O| \cdot |C|\}^2$  of the reference, object and replay beam intensities, and, in the holographic recording method used in the 15' chamber, the maximum possible recorded volume was obtained by reducing the ratio of the object light scattered from a bubble to the reference intensity to the minimum recordable value.

### 3.2 Compensation for Refractive Index Change in Image Space

The optical design of HOLRED relies on the provision of time-reversed optics for the image beam. At the fisheye-chamber interface this cannot be achieved because the relative refractive index of glass to air is greater than that to the hydrogen-neon mixture in the bubble chamber, but the effect can be compensated in replay by reducing the bending power at this interface. In HOLRED, this was achieved by placing another spherical shell in optical contact with the outer fisheye element, thus effectively increasing the radius of the final refracting surface.

Raytracing calculations showed that by this means aberration in the replayed image of a point object could be maintained at  $\lesssim 5 \mu\text{m}$  throughout the illuminated volume in the chamber, whereas without any such compensation, (ie replaying into air through a fisheye of the original thickness), aberrations  $\gtrsim 100 \mu\text{m}$  would be present in images over a large part of the volume.

A consequence of this method of compensation for the refractive index change is the introduction of a non-uniform object-to-image demagnification throughout the chamber volume. A simple calculation shows that a locally paraxial bundle of rays coming from a point at distance  $D$  from the centre of a spherical refracting surface of radius  $R$  and relative refractive index  $\mu$  will retrace to distance  $D'$  from the centre, given by:

$$D = D' \frac{\mu'}{\mu} \frac{1}{\frac{D}{\mu} \left( \frac{\mu' - 1}{R'} - \frac{\mu - 1}{R} \right)} \quad 3.1$$

where  $R'$  and  $\mu'$  are respectively the refracting radius and relative index in replay.

In practice, we had  $\mu$ , (the glass/H-Ne relative refractive index), =  $1.513/1.088 = 1.390$ ,  $\mu' = 1.513$  and  $R = 185 \text{ mm}$ . The replay radius,  $R'$ , was

chosen so as to minimise the image aberrations, and had the value  $R' = 210$  mm. With this value, the relationship between object and image space is shown in Figure 3. The average radial demagnification for events in the holographically recorded volume was  $\sim 2$ ; - an incidental advantage of the existence of this demagnification is that the linear dimensions of the replay machine are correspondingly reduced.

### 3.3 Features of the Design of the Replay Optics

Figure 4 shows how the principles outlined above were realised in the optical design of HOLRED. Light from the dye laser is passed through a beam expansion system to produce a collimated beam of diameter  $\sim 60$  mm, (the size of the exposed region on the holographic film). After being bent into the vertical direction by a  $45^\circ$  mirror, the beam passes through the lens doublet, described in Section 3.1, which produces the converging aberrated beam corresponding to the time-reversed reference beam in the bubble chamber. It then illuminates the film, clamped down against a glass gate positioned at the centre of a (3-component) fisheye lens. The outer element of the fisheye ensemble supports the corrector lens which compensates for the refractive index change. It may be noted that all of these elements are static, so that once the beam is aligned, no further adjustments are made to these components in viewing individual holograms.

After passing through the fisheye, the replay beam is of no more interest as far as replay of the holograms is concerned, and it is transported to a beam dump designed to avoid exposure to personnel. It is now the diffracted image beam which is to be transported to the detector, (either a vidicon or photographic camera), in the replayed chamber space. With the optics described so far, this space (of linear dimension  $\sim 2.5$  m) would be vertically above the fisheye lens. However, in order to keep the image space accessibly low, and also to avoid the mechanical difficulties which would be involved in moving detection equipment in the vertical direction, an additional mirror is placed above the fisheye and its lateral position and angle of tilt adjusted for each replayed event, so that the image always lies in a plane at a fixed height above the floor. Figure 4 also demonstrates the principles of this mirror. Thus the 3 perpendicular movements needed to position the detector at the desired coordinates  $x, y, z$  in replayed image space are supplied in HOLRED by driving the camera on stages along the directions  $Z$  (shown in

Figure 4) and X, (perpendicular to the plane of Figure 4), and by driving the 'Y-mirror' on a stage parallel to direction Z, (also shown in the figure). In addition, the angle  $\theta$  of inclination of the Y-mirror is adjusted in one-to-one correspondence with the Y position, so that the reflected image beam always lies in the horizontal plane.

#### 4. Mechanical, Electrical and Control Aspects of HOLRED

In Figure 4 the HOLRED replay beam optics are seen seated on a flat rectangular base. This base, which is placed on a foam vibration isolation pad, consists of a concrete slab 30 cm thick and  $\sim 3.5 \times 2.5$  m in size and supports the major mechanical installations: the optics, the moving stages and the film drive and positioning assembly. These systems can all be seen in the artist's impression of the machine shown in Figure 5 and the accompanying photograph of HOLRED (Figure 6). The optical system has been fully described above; at this point it need only be noted that, between the exit from the dye laser and the beam expansion system, the replay beam is transported by a system of mirrors which bends it, eventually, through a total angle of  $180^\circ$ . In the rest of this section we describe the most important features of the mechanical and electrical installations and also give some information about the computer control of the machine.

##### 4.1 HOLRED Stages

In Section 3.3 above the principles whereby the replayed image is projected onto vidicon or photograph detectors were described. The implementation of these ideas can be seen in Figure 5 and 6. The Z-stage rides on rails attached to the concrete base, while the X-stage rails sit on the Z-stage and straddle the replay beam transport optics (enclosed in tubing). The detectors are mounted on a further stage, (not previously mentioned), which can rotate about a vertical axis. This stage, the 'R-stage', has two purposes: first, by swinging through a large angle, ( $\sim 90^\circ$ ), the vidicon and photographic detectors can be interchanged as desired by the operator; and, secondly, events can be viewed with the detector plane non-parallel to the z axis so that, in principle, tracks can be viewed in focus along their length regardless of their angles of dip with respect to the xy plane. (In practice, almost all particles are emitted from interaction points with dip angles  $\lesssim 20^\circ$ ).

In Figures 5 and 6 two vidicon cameras can be seen. These provide views of events with two different magnifications; one camera, which is lensless, displays the image with unit magnification with respect to image space, and the other is equipped with an objective lens providing a demagnification of  $\sim x3$ .

The operator is given manual control over all 4 stages (X, Y, Z and R) by means of tracker ball and control wheel so that the optimum orientations of events can be chosen for examination on the TV monitor and subsequent photography.

Figures 5 and 6 also show the Y-stage control. This is positioned vertically above the fisheye lens and consists of a stage which moves the 'Y-mirror' back and forth horizontally in the Z direction. The tilt of the mirror is adjusted by means of a cam driven from the Y-stage rails so that the image always lies in a horizontal plane at the height of the cameras.

The three linear stages are equipped with digitisers with least counts of  $17 \mu\text{m}$  (X and Z) and  $2 \mu\text{m}$  (Y). This accuracy is more than enough to position the detectors at points where interesting phenomena are expected; it also suffices for the use of HOLRED to make measurements of track lengths and interaction points, although more accurate measurements are in general available by projecting the photographs taken with HOLRED in conventional 2-dimensional bubble chamber film measurement machines.

It may be noted that no chamber-based fiducial marks are available in the system used for holographic recording in the 15' chamber. However, a perfectly satisfactory system of absolute calibration of HOLRED is available. This is achieved, in the first place, by using Eq 3.1 to predict the distance from the fisheye in image space at which an object at the laser entry point in bubble chamber space will be replayed. The replay beam is then focused to a point at this distance from the fisheye. This then ensures that the position of all images can be calculated from known object positions using only Eq 3.1 and the knowledge that the angular coordinates in a system concentric with the fisheye are unchanged in the object-to-image transformation. The calibration is then effected, assuming only orthogonality of the 3 stage drive coordinates and an accurate knowledge of the stage least counts.

The stepping motors and precision encoders needed for the linear stages were obtained from Siemens AG, with the motors selected to the specification that the time to drive between any two points in replayed image space should not exceed 30 s.

#### 4.2 Film Transport and Positioning Systems

The specification given for HOLRED in Section 1 implies two separate demands on the film transport system: first, that it should be possible to drive from one frame to another in rolls of  $\sim 1,000$  holographic exposures at reasonable speed; and second, that the film can be positioned to within an accuracy of  $\sim 30 \mu\text{m}$  under the fisheye. In this section we describe how these demands are fulfilled.

The spools carrying the holographic film can be easily seen in Figures 5 and 6. The 70 mm sprocketed film is driven between these spools using a capstan drive located adjacent to the fisheye, with additional take-up drive applied to the spools. A vacuum system supplies tension to the film under the fisheye. Two drive speeds are available, 1 cm/sec and 40 cm/sec. The expected rate for occurrence of interactions of interest on the holographic film, assuming ideal conditions during data-taking was 1 per 4 frames, though in practice the rate obtained was a factor  $\sim 5-10$  less than this. However, this still implies a reasonably low access time between frames of interest.

In order to position a desired frame under the fisheye, a vidicon camera is focused on the moving film and the image displayed on a monitor forming part of the operator's control console. The operator can stop the film drive when the desired frame is approaching the film gate and perform an initial rough positioning of the film under the fisheye. The film is then clamped down onto the glass film gate by vacuum suckdown, and positioned accurately by alignment of two of the three camera-based fiducial marks, (described in Section 2.1). These marks are illuminated by a light source and their images focused onto two further vidicon cameras, monitored in the control room. The optical system used to view the fiducial marks utilises 'Selfoc' light-guide lenses to transport the light collected out of the congested region under the fisheye to the vidicon cameras. In order to position the film so that the fiducial images appear in their correct places on the TV monitor, the film

gate was mounted on a high precision stage so that the clamped-down film could be moved in fine steps in two perpendicular directions in the film plane and about one axis perpendicular to the film plane. The precision stage and motors used for these movements were obtained from Microcontrole SA. In case there is residual inaccuracy in the whole resetting procedure from camera fiducials, via their film imprints, to the HOLRED vidicon camera positions, final adjustments to the film position can be made by optimising the replayed quality of actual track images, again using the three film-gate movements.

#### 4.3 Control and Operation of HOLRED

The discussion given in the previous sections has given some indication of the overall mode of operation of HOLRED. This procedure is now summarised, and at the same time the computer control aspects of the machine are described,

The coordinates of events of interest, obtained by digitisation and stereoscopic reconstruction of measurements on the conventional photographic cameras, are stored on a database on a VAX 780 computer. The HOLRED operator, interacting with a program running on an LSI11 computer, can access the VAX database via a communications link to find the frame number and coordinates of the next frame of interest. The film is then driven to its correct position and the fiducial alignment carried out by the operator, as described in the previous section. The three stages (X, Y and Z) are then driven to the image space coordinates of the event of interest under computer control, using CAMAC to interface the LSI11 to the stage drive electronics. The operator can then view the event on the TV monitor, selecting either high or low magnification. Using the tracker ball and wheel controls, it is then possible to examine aspects of interest and select the best viewing positions by manual control of the four stages - the three translational stages and the rotational stage which allows the camera to be rotated about a vertical axis. If a photograph of the event is desired, the photographic camera is then positioned automatically so that the recording film is in the same place as the last-viewed vidicon image and a photograph is then taken. The required exposure of the photographic camera is determined automatically from measurement of the light level at the camera. Finally, the camera is exposed to an LCD display containing information about the event, (such as frame



number), and this information, together with new fiducial marks, is recorded on the HOLRED output film. The VAX database is updated with a record of the actions performed.

## 5. Results and Discussion

HOLRED is currently being used for the analysis of a sample of 60,000 holograms from the FERMILAB 15' chamber which are expected to produce  $\sim$  1000-2000 holographically recorded events. It has already been used for the analysis of a preliminary sample of 50,000 holograms in which the event rate was low and the main aim was the study of holographic quality. Typical results are shown in Figure 7, in which the holographic recordings of events (Figures 7a,7c) can be compared with the corresponding photographic recordings (Figures 7b,7d respectively). The advantage of the availability of a high resolution view in clarifying activity near the interaction point can readily be seen.

In this paper we have described the reasons why holography is of use in current studies of particle interactions in bubble chambers, the specification for a machine to analyse holograms taken in large bubble chambers has been discussed, and we have described the fulfilment of this specification, in HOLRED, for the specific holographic arrangement in the 15' chamber. More generally, HOLRED can be considered as an example of a machine for bulk analysis of large volume high resolution holograms. Other applications of this type of holography have been reported, for instance in the fields of remote visual inspection of nuclear fuel rods<sup>[13]</sup> and analysis of explosion fragments<sup>[14]</sup>. Continuing improvements in holographic technique make it likely that further applications will appear in the future. Although the requirements for replay facilities are rather dependent on each specific application, and in particular on the holographic recording geometry, it is possible that, in HOLRED, solutions exist to many of the problems which will be encountered in the design and construction of such machines.

## Acknowledgements

The authors are indebted to technical staff in several institutions for their help in constructing HOLRED. In particular, thanks are due to W J Cheape and E C Isherwood of Birmingham University, and F Jacob and P Mace of Rutherford

Appleton Laboratory. We also thank the following institutions for providing funds and equipment for the construction of the machine:

University of Birmingham, CEN Saclay, CERN, Imperial College London, Max Planck Institut, Munich, Oxford University, Rutherford Appleton Laboratory and ULB Brussels.

### References

1. W T Welford, Appl Opt 5 (1966) 872.
2. A P Komar, M V Stabnikov and B G Turukhano. Proc of the Seminar on Bubble Chamber Methods of JINR and CERN Physicists, JINR, Dubna (1965) p7.
3. D Crennell, C M Fisher and R L Sekulin, Nucl Instr and Meth 158 (1979) 111.
4. A Hervé et al, Nucl Instr and Meth 202 (1982) 417.
5. H Bjelkhagen et al, Nucl Instr and Meth 227 (1984) 437.  
H Bjelkhagen et al, Nucl Instr and Meth 220 (1984) 300.
6. H Drevermann, K K Geissler and K E Johnsson, Nucl Instr and Meth A242 (1985) 65.  
P R Hobson et al, Nucl Instr and Meth A239 (1985) 155.  
M Barth et al, Nucl Instr and Meth 226 (1984) 349.
7. M W Peters and R J Cence, in: Photonics Applied to Nuclear Physics: 2, Nucleophot, Strasbourg (1984), CERN 85-10, p95.  
R Naon et al., to be submitted to Nucl. Instr. and Meth.
8. T Kitagaki, in: Photonics Applied to Nuclear Physics: 2, Nucleophot, Strasbourg (1984), CERN 85-10, p99.
9. P R Nailor, ibid, p83.
10. G Harigel, in: Proc Second Topical Seminar on Perspectives for Experimental Apparatus at Future High Energy Machines, San Miniato, (1986), Nucl Instr and Meth A257 (1987) 614.
11. See, for example, H M Smith, "Principles of Holography", John Wiley and Sons, (1975), p238.
12. ibid, p143.
13. R Glanville et al, in: Proc Electro-Optics/Laser International '84 UK, Brighton, publ Cahners Exhibitions Ltd (1984), p314.
14. H Royer, in: Proc Conf. on Progress in Holographic Applications, Cannes, SPIE 600 (1985), 127.

## Figure Captions

- Figure 1** Sectional view of the Fermilab 15' Bubble Chamber. The optical scheme used for making holographic recordings is indicated.
- Figure 2** Principles of image reconstruction for holograms made in the Fermilab 15' Bubble Chamber, used as the basis of the design of HOLRED.
- Figure 3** Mapping of the inside surface of the Fermilab 15' Bubble Chamber showing the original chamber and - (the smaller shape) - the same volume reconstructed with the optics of HOLRED. The non-uniform demagnification on replay arises from the refractive index change (H-Ne to air) between recording and replaying holograms. Points L, L<sub>R</sub> are the original and reconstructed laser entry parts to the chamber, and point C designates the holographic camera position at the fisheye centre. In the original chamber the distance LC was  $\sim 4.1$  m.
- Figure 4** Vertical section through the fisheye centre showing optics of the replay and image beams on HOLRED.
- Figure 5** Artist's impression of HOLRED showing the main optical and mechanical features of the machine. The nearer end contains the film drive and positioning assemblies, the fisheye lens and the "Y-mirror" assembly for projecting the image in a horizontal plane. At the further end can be seen the X and Z stages which ride on rails, and the photographic camera positioned for recording an image. The positions of the photographic and vidicon cameras can be interchanged by rotating the stage on which they are mounted through 90°.
- Figure 6** Photograph of HOLRED, looking towards the film-drive, fisheye and Y-mirror assemblies. The X-stage is seen in the foreground. The argon ion and dye lasers are seen on the left-hand side of the machine; the beam from the dye laser is turned through 180° and approaches the fisheye lens along the central axis of the machine, (enclosed in black tubing).

Figure 7

Comparison of holographic reconstruction on HOLRED of neutrino interactions in the Fermilab 15' bubble chamber (a,c) with corresponding conventional views of the same events (b,d respectively). Careful examination of the two uppermost tracks in the holographic reconstruction (a) has revealed that they do not come from the same interaction point as the other tracks; this fact is entirely obscured in the conventional photograph (b). The achievement of a substantial improvement in resolution in going from conventional to holographic optics is readily seen in both events; the relative magnifications of the holographic and photographic views are  $\sim 1:1$  for a:b and 1.5:1 for c:d. In the holographic views the viewing camera has been focused on one particular outgoing track in each holographic reconstruction; - for instance in (c), the uppermost track from the primary production point has been chosen. The other tracks, which in general will have different dip angles with respect to the one chosen to lie in the viewing camera film plane, then become defocused as they leave the ( $\sim 1$ cm deep) focused region.

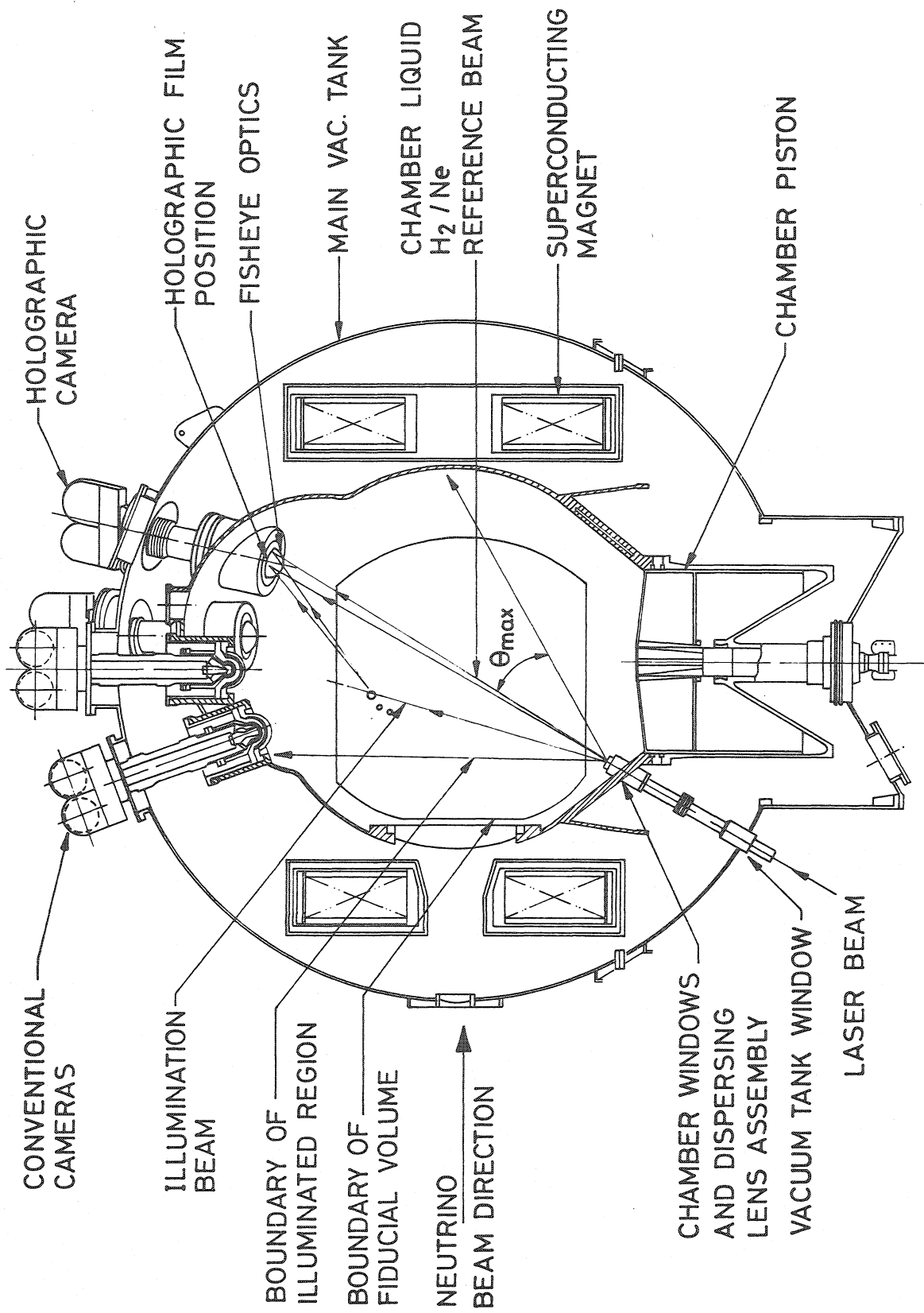


Fig. 1

# HOLOGRAPHIC REPLAY - REAL IMAGE

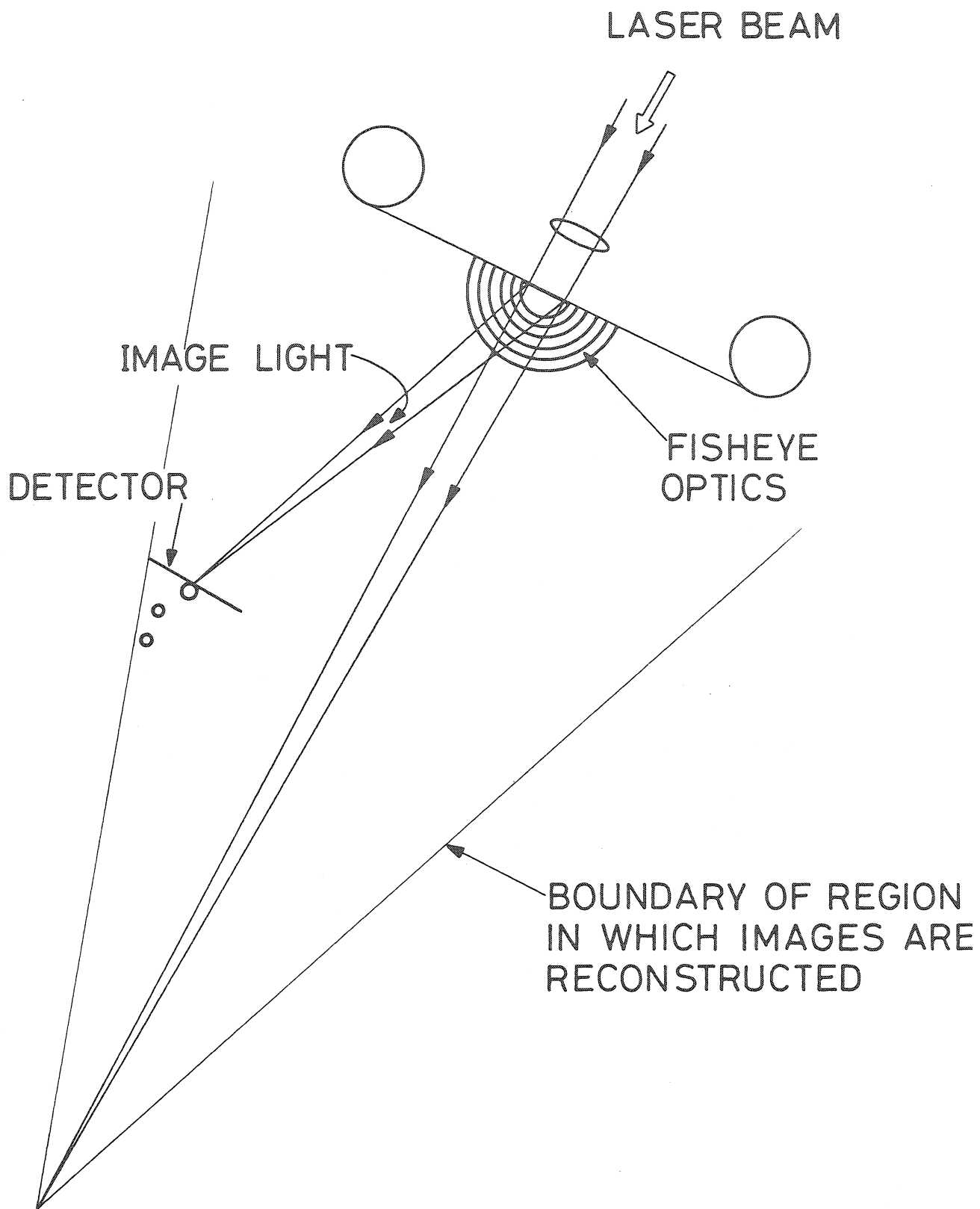


Fig. 2

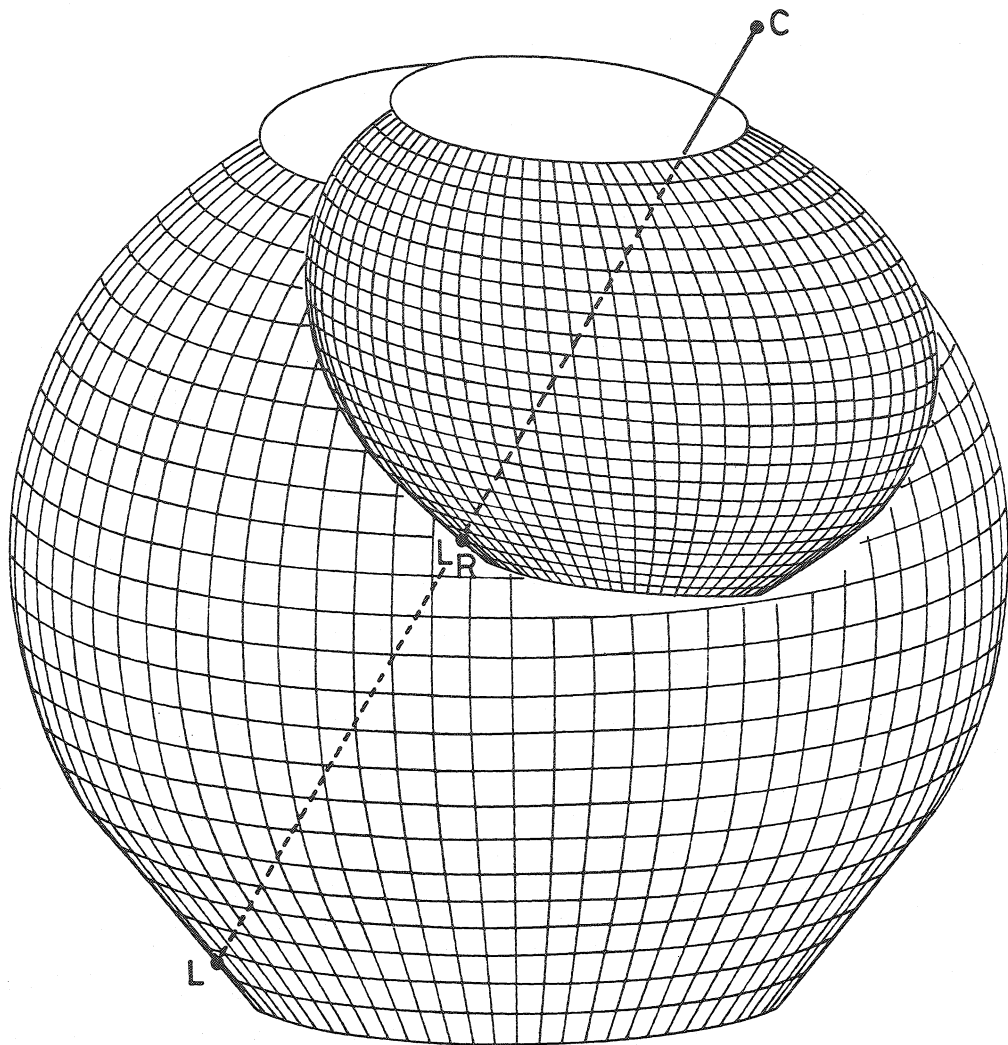


Fig. 3

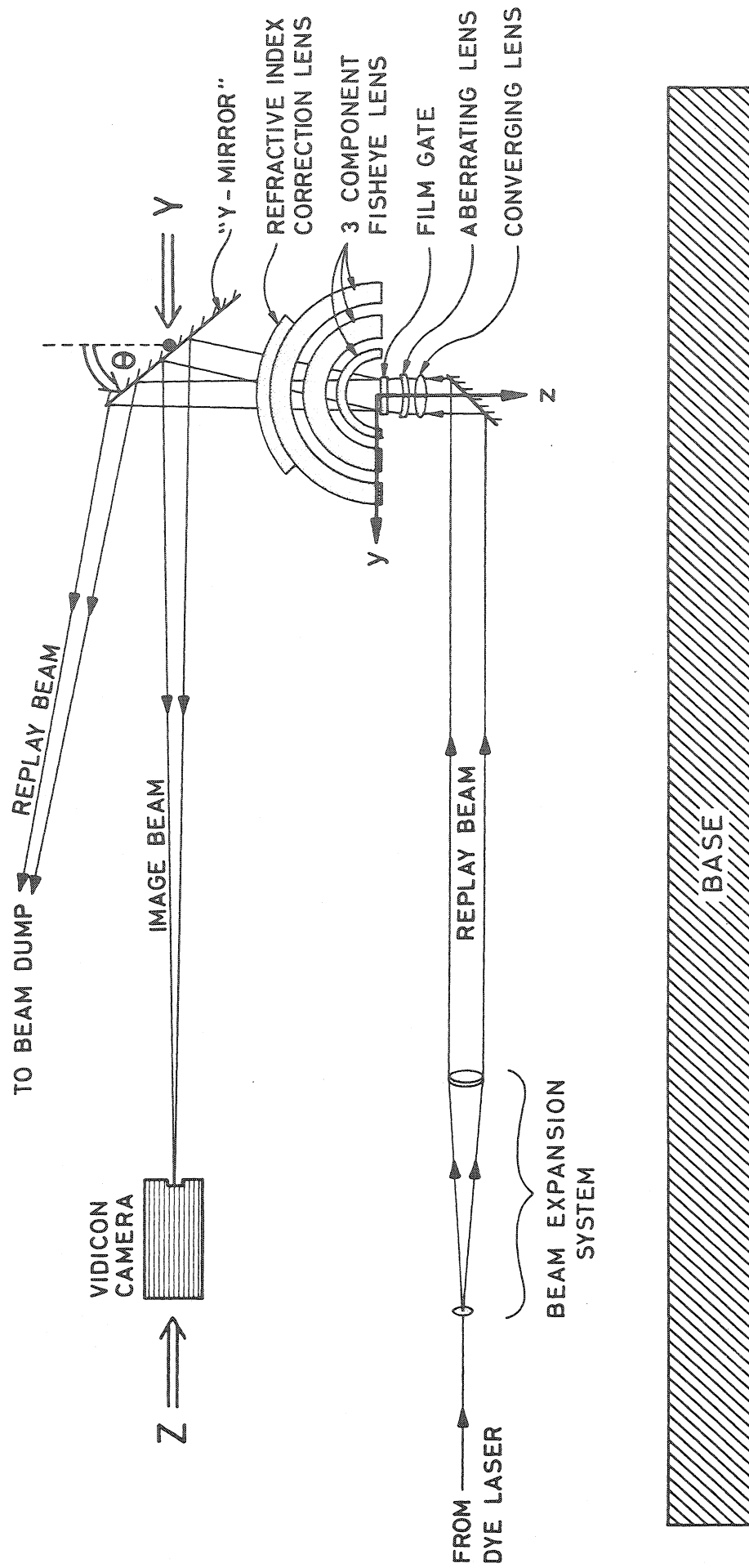
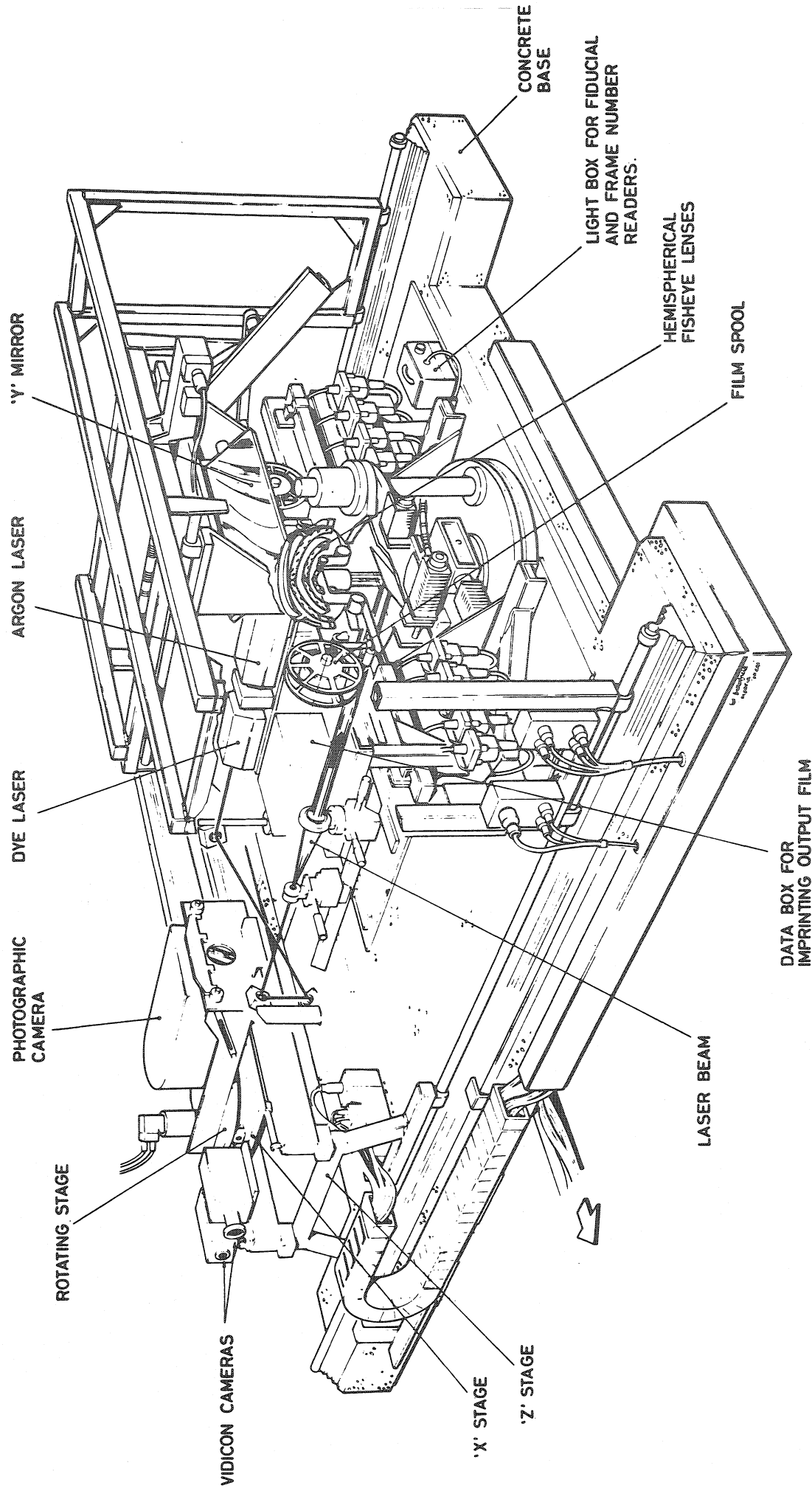


Fig. 4





"HOLRED"

Fig 5

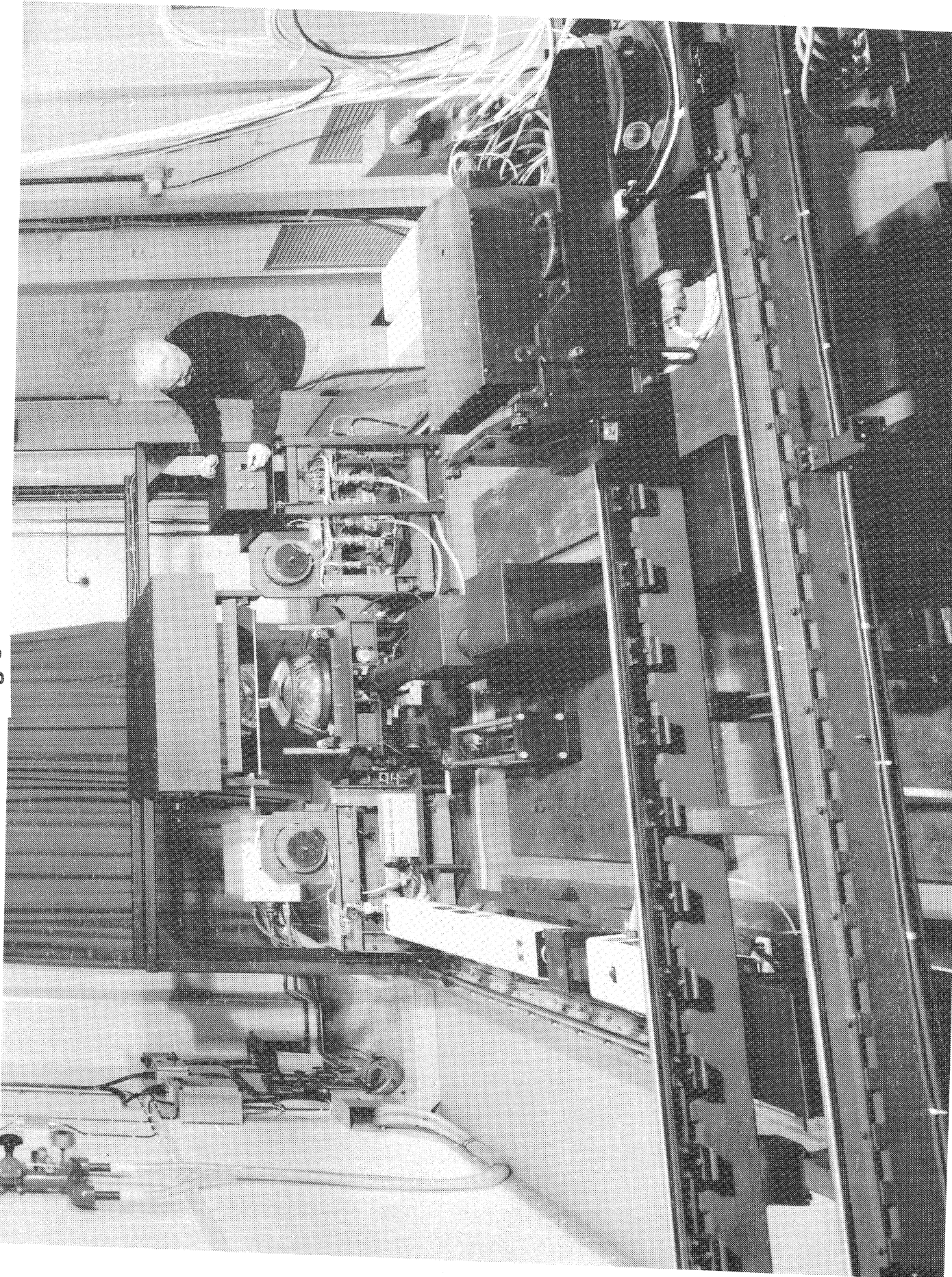


Fig 6

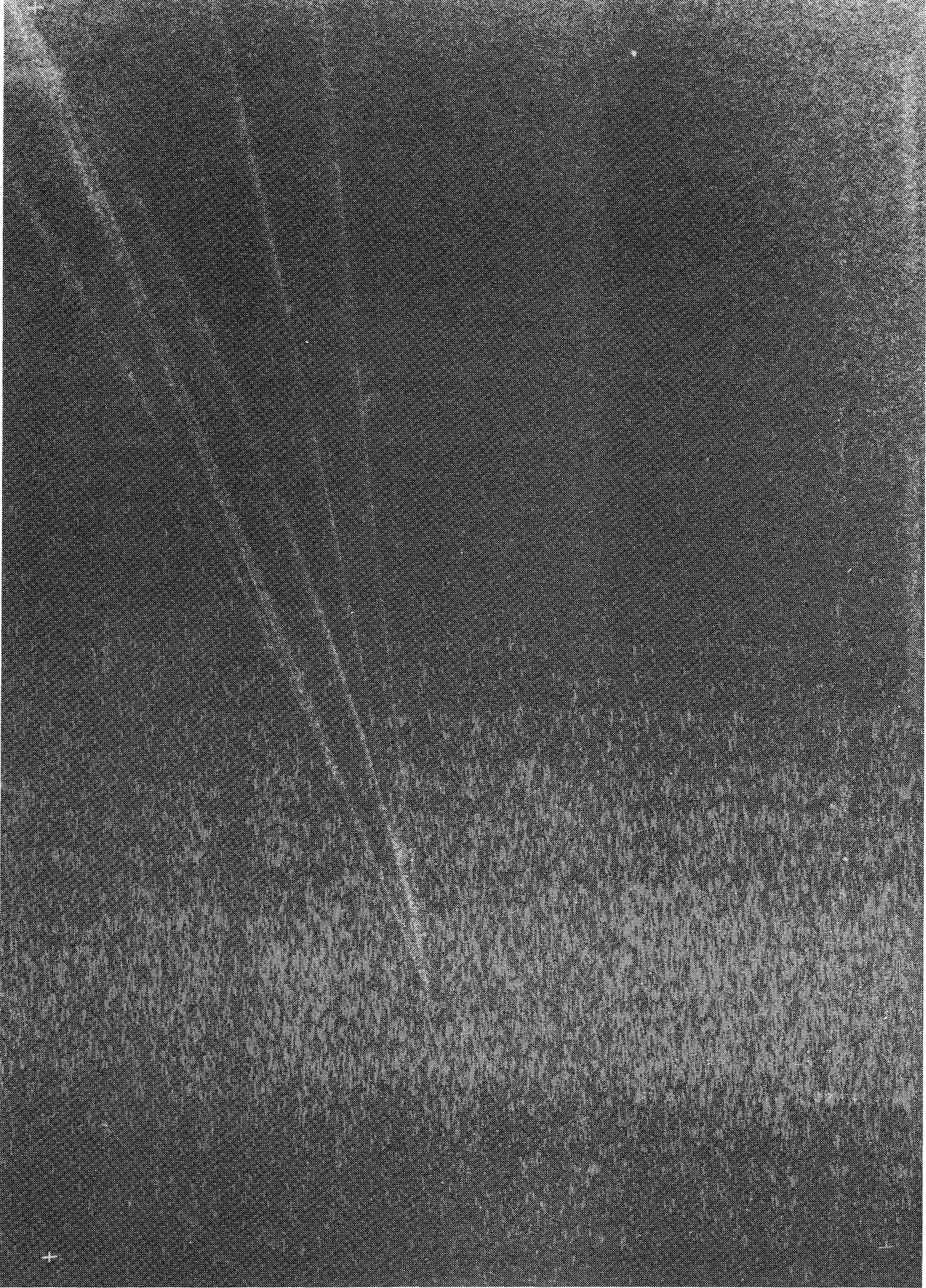
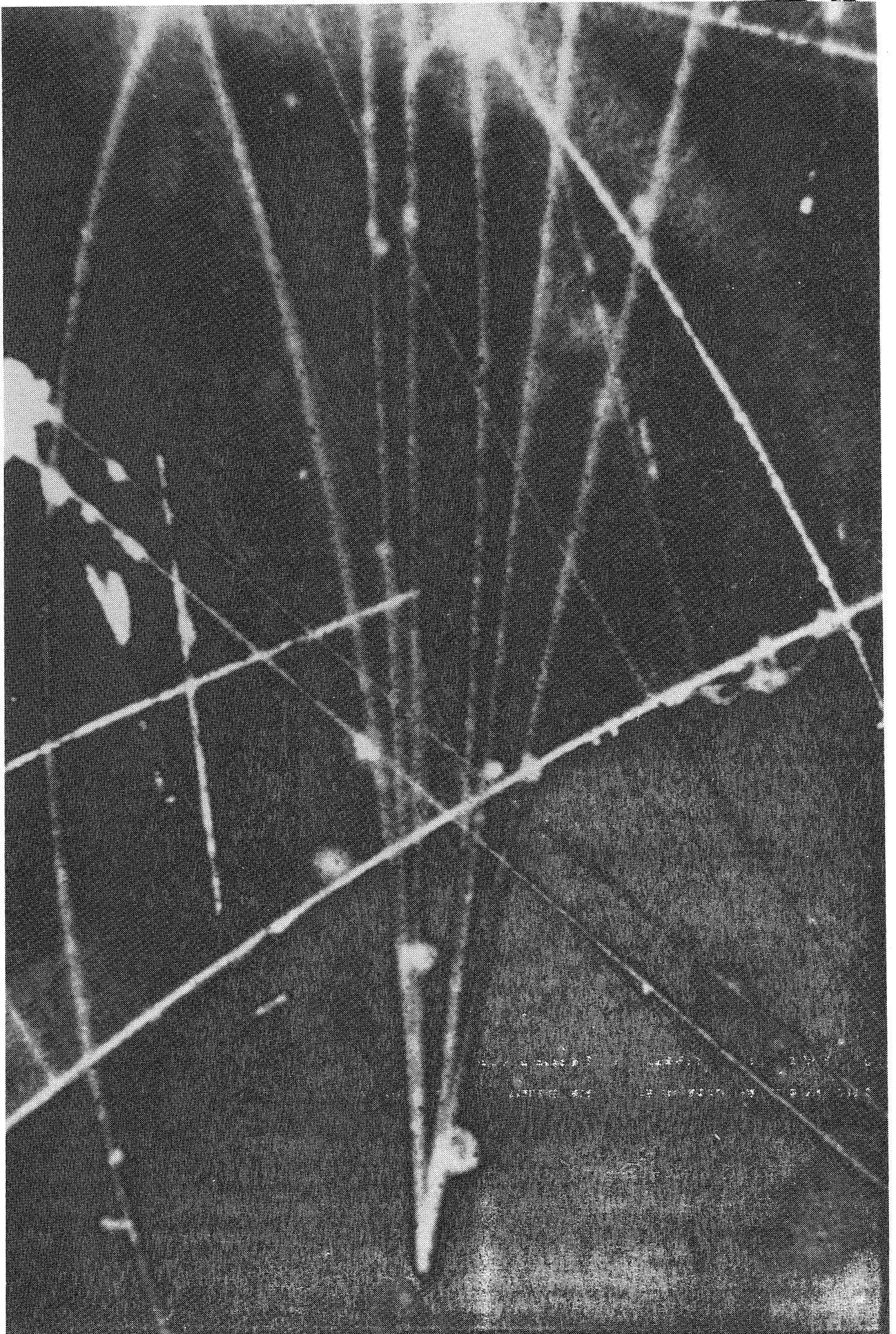


Fig 7a



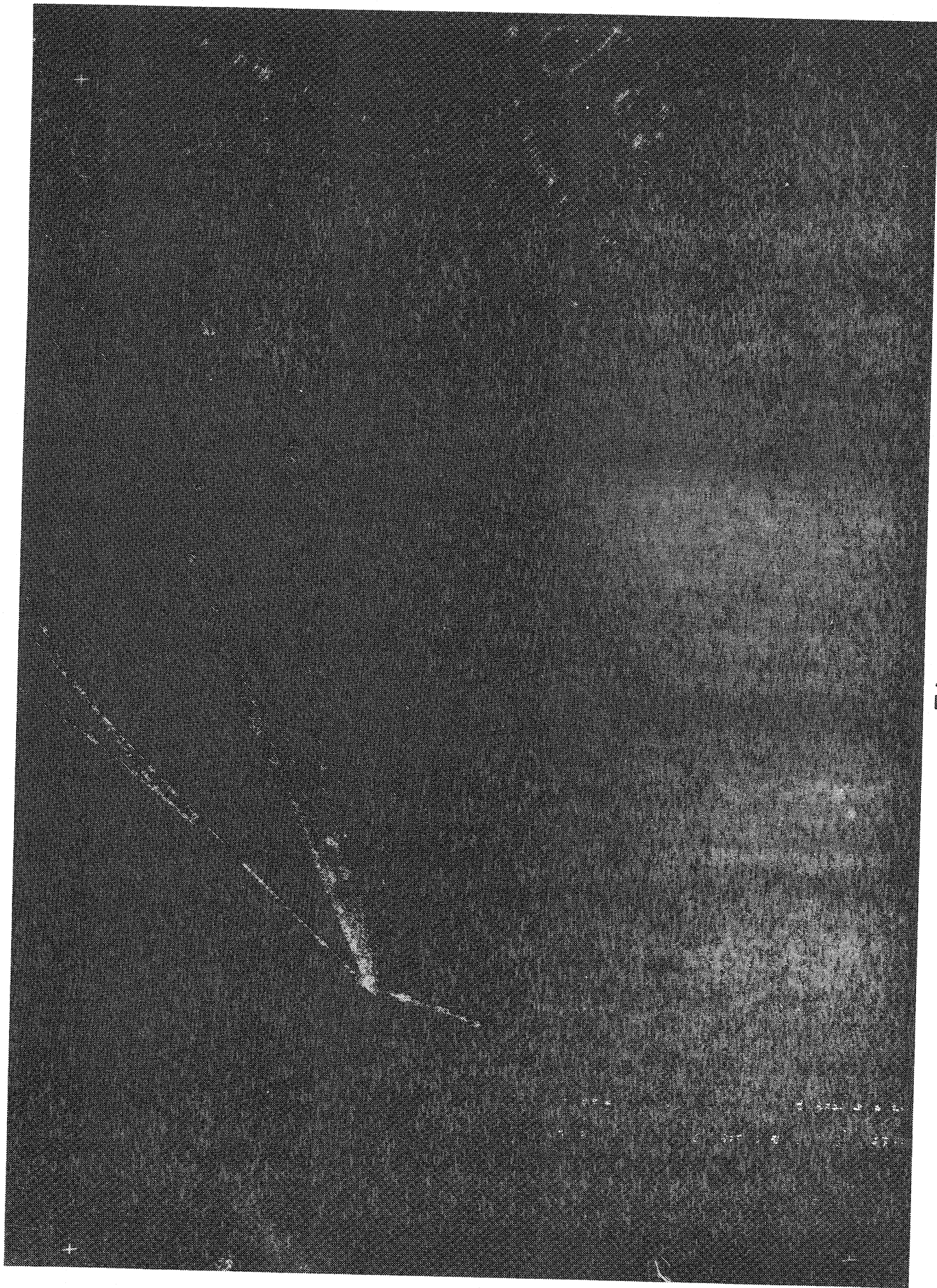


Fig 7c

